Evaluation of a Survey-Grade, Long-Range Uas Lidar System: a Case Study in South Texas, USA

Conference Paper · July 2018

DOI: 10.1109/IGARSS.2018.8517340

CITATION
1

READS
413

3 authors:

Michael J Starek
Texas A&M University - Corpus Christi
100 PUBLICATIONS **913** CITATIONS
SEE PROFILE

Tianxing Chu
Texas A&M University - Corpus Christi
44 PUBLICATIONS **611** CITATIONS
SEE PROFILE

David Bridges
Texas A&M University - Corpus Christi
40 PUBLICATIONS **257** CITATIONS
SEE PROFILE

EVALUATION OF A SURVEY-GRADE, LONG-RANGE UAS LIDAR SYSTEM: A CASE STUDY IN SOUTH TEXAS, USA

Michael J. Starek[1,2], *Tianxing Chu*[1], *David Bridges*[2]

[1]Conrad Blucher Institute for Surveying and Science, Texas A&M University-Corpus Christi, Corpus Christi, TX 78412

[2]School of Engineering and Computing Sciences, Texas A&M University-Corpus Christi, Corpus Christi, TX 78412

1. INTRODUCTION

Over recent years, light detection and ranging (lidar) sensor technology has rapidly evolved and miniaturized. The reduced sensor size and weight have opened more doors for lidar sensors to be carried onboard unmanned aircraft systems (UASs) [1]. Compared with traditional airborne lidar mapping, UAS platforms offer more flexibility in terms of flight design and data collection, rapid response capabilities, and potentially cost at local mapping scales.

UAS-based lidar studies have primarily been focused on monitoring vegetation structure, simultaneous localization and mapping (SLAM) and so forth. A comparison between UAS and terrestrial laser scanning (TLS)-derived plant height for crop monitoring was made in [2]. Descriptive statistics derived from polygon grids were analyzed and a correlation $R^2 = 0.91$ was found in plant height derived from both methods. In [3], a lidar-based perception and guidance system was built on a helicopter to perform obstacle detection and avoidance, terrain following, and close-range inspection, and a high success rate was claimed by the authors.

Structure-from-Motion (SfM) / Multi-View stereo (MVS) photogrammetry represents an alternative to airborne lidar to derive 3-D point cloud data. It relies on adequate image overlap to extract key point correspondence and collinearity to reconstruct the 3-D scene. This single return solution is sometimes susceptible to false parallax induced from moving vegetation between overlapping images (for instance due to wind) and to poor feature correspondence in areas where the image texture is highly uniform [4], [5]. One advantage of using lidar is it uses pulsed ranging technique and many lidar systems provide multiple return detection capability. This multi-return capability has enabled lidar to be widely applied to forestry inventory surveys among other applications because it allows for canopy and below canopy measurement.

A mini-UAS-borne lidar system was built in [6], and its applicability for fine-scale mapping was validated in terms of tree height estimation, pole detection, road extraction, and digital terrain model refinement. A more recent study in [7] developed a lidar-hyperspectral image fusion method in treated and controlled forests with varying tree density and canopy cover to classify vegetation and measure 3D structure. It was claimed that the fusion method performed better than either data type alone at the study site in the southwestern USA.

In this paper, initial results on the testing and evaluation of a single-rotary UAS integrated with a long-range, multi-return lidar sensor is presented. Testing was performed at an airfield in South Texas, USA. The study primarily focuses on: 1) description of the platform and enabling technology (i.e., lidar/IMU/GPS) of the fully integrated UAS solution, 2) sensor calibration and initialization (e.g., boresight calibration and IMU initialization), and 3) description of the geospatial surveying, data processing and analysis.

2. SYSTEM SETUP AND INITIALIZATON

The UAS platform used in the study is a single-rotary vertical take-off and landing (VTOL) Pulse Aerospace Vapor 55 (Table 1). A Northrop Grumman LITEF µIMU was initially mounted with the system, however, it was found that one of the gyros was interfered at certain low frequencies in the 20 Hz range. These unfortunately are the exact frequencies that the Vapor 55 emits. Therefore, a KVH 1750 IMU was used as an alternative IMU. As shown in Fig. 1, a RIEGL VUX-1LR lidar system (Table 2) and KVH 1750 IMU (Table 3) integrated by Phoenix Lidar Systems were attached underneath the platform.

Table 1. Pulse Aerospace Vapor 55 specifications [8]

Gross weight	24.95 Kg
Useful load (battery & payload)	15.42 Kg
Allowable payload (with full endurance)	< 4.99 Kg
Max cruise endurance (with full payload)	60 Minutes
Max hover endurance (with full payload)	45 Minutes

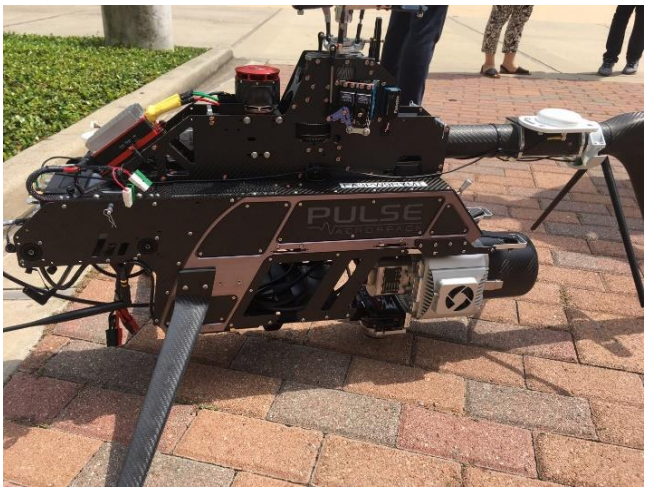

Figure 1. Pulse Aerospace Vapor 55 platform with lidar/IMU sensors onboard.

Table 2. RIEGL VUX-1LR specifications [9]

Laser properties	Class 1 (eye safe), 1550 nm
Min range	5 m
Field of view	330°
Max effective measurement rate	750,000 meas./s
Max scan speed	200 scans/s
Max operating flight altitude	530 m
Laser beam footprint	50 mm @ 100 m, 150 mm @ 250 , 250 mm @ 500 m
Max range @ target reflectivity 60%	1350 m
Max range @ target reflectivity 20%	820 m
Accuracy	15 mm @ 150 m (1σ)
Multi-echo detection	10+ returns

Table 3. KVH 1750 IMU specifications [10]

Gyro bias offset (25°C)	±2°/hr
Angle random walk (25°C)	≤0.012°/√hr (≤0.7°/hr/√Hz)
Gyro bias instability (25°C)	≤0.1°/hr, 1σ (max), ≤0.05°/hr, 1σ (typical)
Bias instability (constant temp)	<0.05 mg, 1σ
Velocity random walk (25°C)	≤0.12 mg/√Hz (0.23 ft/sec/√hr)

Fig. 2 shows Vapor 55 system setup and flight details. Before a flight is conducted, travel speed, flight height, direction and trajectory are planned and transmitted to the platform via ground control software tuned for the Vapor 55 running on the ground control station (GCS). Flight controls, i.e. an older Sony Playstation joystick, as shown in Fig. 2 (b), are also provided in a manual operation mode for precise guidance during taking off and landing stages. As part of flight design protocol for the system, two "figure eight" hippodromes are added to each flight mission at the start and end of the survey lines prior to landing to initialize the IMU sensors and improve inertial post-processing.

High-accuracy GPS/IMU trajectory can be generated by using NovAtel Inertial Explorer software. Georeferenced point cloud data can then be created from loading in GPS/IMU trajectory with raw laser files in Phoenix Lidar Systems Spatial Fuser software.

In addition, this system also enables a real-time direct georeferencing solution and the results shown subsequently are based on the real-time solution. Fig. 3 illustrates real-time point cloud results, as opposed to high-accuracy post-processed results, at Texas A&M University-Corpus Christi campus visualized in Phoenix Lidar Systems Spatial Explorer software. Many structural misalignment errors can be noticed in this real-time solution.

It is worth noting that the lever arm offsets between the IMU measurement center and global navigation satellite system (GNSS) antenna phase center must be determined as well as boresight calibration parameters to orient the sensor frame relative to IMU frame prior to undertaking any surveying tasks.

Figure 2. Vapor 55 system setup and flight details. (a) platform setup by TAMUCC students; (b) side view of the Vapor 55 ground control station (GCS) and flight controls; (c) ground control software running on GCS; and (d) platform flying in the sky.

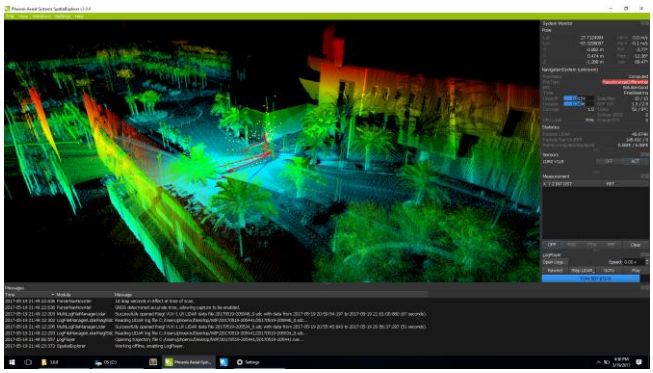

Figure 3. Point cloud results at Texas A&M University-Corpus Christi campus using the Vapor 55 and RIEGL VUX-1LR scanning system visualized in Phoenix Lidar Systems Spatial Explorer software.

3. INITIAL RESULTS

Initial flights have been undertaken at Alfred C 'Bubba' Thomas Airport (28.0385669°N, -97.5425013°W) on May 17, 2017 (without payload), and July 22, 2017 (with payload), in Sinton, TX. The GPS/IMU trajectory was processed by NovAtel Inertial Explorer in a tightly-coupled manner (Fig. 4). The platform performed two hippodromes at the beginning and end for IMU initialization, and continued in parallel flight lines over the airport for data collection. The endurance times listed in Table 1 are based on ideal conditions, however, in practice a max of 35 minutes was experienced in our study. This flight was flown for approximately 20 minutes of time. Fig. 5(a) shows a real-time point cloud overview of the airport at 70 m above ground level. The yellow arrow indicates the airport runway. Vegetation can also be observed by the runway. Fig. 5(b) provides a closer side view near the vegetation area and power lines can be distinguished as indicated by the yellow arrow. Offset in the point cloud is apparent due to real-time direct georeferencing of the range measurements from the lidar sensor.

A recent survey on January 5, 2018, was conducted to perform a new boresight calibration of the installed IMU. Perpendicular and overlapping fight lines were flown over a hangar and runway to perform the calibration by assessing systematic misalignments in scan lines on static structures. Results of the calibration are shown in Table 4. Current efforts are focused on a rigorous analysis of lidar horizontal and vertical accuracies and developing a “best practices” for data acquisition to maximize flight time using the system.

Table 4. Results of lidar sensor boresight calibration flight

	X	Y	Z
Translation (m)	0.000	0.000	0.188
Rotation (°)	0.098	-179.999	-0.064

Figure 4. GPS/IMU trajectory at the Alfred C 'Bubba' Thomas Airport (28.0385669°N, -97.5425013°W) in Sinton, TX (processed by NovAtel Inertial Explorer).

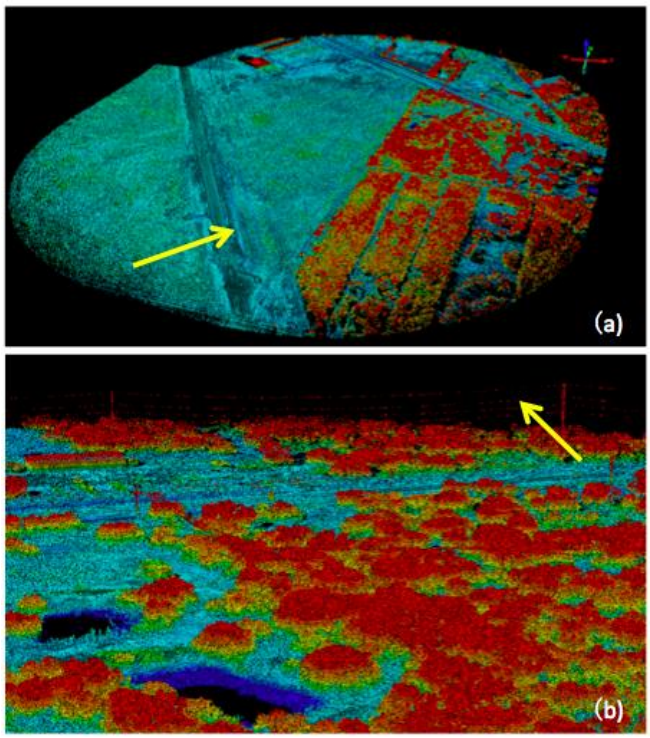

Figure 5. Point cloud results at the Alfred C 'Bubba' Thomas Airport in Sinton, TX. (a) Overview of the scanned area in a real-time solution mode; and (b) side view of the vegetated area in the airport.

4. ACKNOWLEDGMENT

The authors are grateful to Maurice Griffin from the Lone Star UAS Center at Texas A&M University-Corpus Christi (TAMU-CC) for serving as pilot in command during the UAS flight operations.

5. REFERENCES

[1] M. Starek and J. Jung, "Lidar's Next Geospatial Frontier: The State of Lidar for UAS Applications," *GIM International*, vol. 29, pp. 25-27, 2015.

[2] G. Bareth, J. Bendig, N. Tilly, D. Hoffmeister, H. Aasen, and A. Bolten, "A comparison of UAV and TLS-derived plant height for crop monitoring: Using polygon grids for the analysis of crop surface models (CSMs)," *Photogrammetrie Fernerkundung Geoinformation*, vol. 2016, no. 2, pp. 85-94, 2016.

[3] T. Merz and F. Kendoul, "Beyond visual range obstacle avoidance and infrastructure inspection by an unmanned helicopter," in *Proc. IEEE/RSJ International Conference on Intelligent Robots and Systems (IROS 2011)*, September 2011.

[4] T. Chu, R. Chen, J. A. Landivar, M. M. Maeda, C. Yang, and M. J. Starek, "Cotton growth modeling and assessment using unmanned aircraft system visual-band imagery," *J. Appl. Remote Sens.*, vol. 10, no. 3, p. 036018, 2016.

[5] C. Stanton, M. J. Starek, N. Elliott, M. Brewer, M. M. Maeda, and T. Chu, "Unmanned aircraft system-derived crop height and normalized difference vegetation index metrics for sorghum yield and aphid stress assessment," *J. Appl. Remote Sens.*, vol. 11, no. 2, p. 026035, 2017.

[6] Y. Lin, J. Hyyppä, and A. Jaakkola, "Mini-UAV-borne LIDAR for finescale mapping," *IEEE Geosci. Remote Sens. Lett.*, vol. 8, no. 3, pp. 426–430, 2011.

[7] T. Sankey, J. Donager, J. McVay, and J. B. Sankey, "UAV lidar and hyperspectral fusion for forest monitoring in the southwestern USA," *Remote Sens. Environ.*, vol. 195, pp. 30-43, 2017.

[8] http://www.pulseaero.com/uas-products/vapor-55, accessed January 2018.

[9] http://www.riegl.com/uploads/tx_pxpriegldownloads/ RIEGL_VUX-1LR_Datasheet_2017-09-01.pdf, accessed January 2018.

[10] https://www.kvh.com/~/media/A7B9D37D82D24B129A221637D7CDE439.aspx, accessed January 2018.